PARTICLE TRACKING IN FLUORESCENT MICROSCOPY IMAGES IMPROVED BY MORPHOLOGICAL SOURCE SEPARATION

Nicolas Chenouard[1], Isabelle Bloch[2], Jean-Christophe Olivo-Marin[1]

[1]Institut Pasteur, Unité d'Analyse d'Images Quantitative; CNRS URA 2582, Paris France
[2] TELECOM ParisTech, CNRS UMR 5141 LTCI, Paris, France

ABSTRACT

Particle detection and tracking methods generally assume a simplistic image model that is rarely valid when imaging biological processes in fluorescence microscopy. The tracking task may become nearly impossible when complex biological structures are visible and interfere with the signal of interest. To address this limitation we have adapted a source separation technique based on sparsity principles to the characteristics of fluorescent biological images. Since it allows the discrimination of objects with different morphologies, we present an approach to detect and track particles that exploits its results. The tracking algorithm resolves particles that temporarily aggregate by exploiting the proposed model of image. We prove in a real case the ability of the method to track numerous particles in a complex and dynamic background, something which was not feasible until now, hence offering new tools to document interactions between cellular compartments.

1. INTRODUCTION

Particle tracking has become a reference tool to study and understand intracellular processes by taking advantage of recent developments in live microscopy techniques. The classical paradigm of particle tracking is a detection step, followed by a linking procedure. Detection procedures are generally either based on a filtering process, such as wavelet detectors [1], or on a template matching, such as Gaussian mixture fitting [2] (read [3] and references therein for a review). Approaches relying on the Bayesian modeling of the tracking have attracted lots of attention and are nowadays commonly used [4, 5, 6]. Their principle is to estimate a statistical model of trajectories in order to discriminate the most likely association between tracks and detections. While Bayesian methods were primarily designed to exploit the kinetics of targets, the image information has been also introduced to improve the robustness of the association procedure. Methods such as [4] and [5] have used the local intensity as a feature, and more recently we have proposed in [7] to incorporate a more complete description of the image model in the association score.

Generally, the underlying image model for the detection process and the tracking step is assumed to be the addition of the targets intensities to a locally constant background and a random acquisition noise. However the background assumption is rarely valid when imaging biological systems in fluorescence microscopy. Both the intracellular and extracellular areas are very crowded environments and the labeling is generally not strictly specific to the targets. Hence structures such as membranes or filaments emit photons which create a

structured dynamic background. These structures corrupt the particle detection process since they can be misinterpreted as signals of interest. The presence of such spurious detections may result in false associations of tracks and creation of non existent trajectories. Moreover the erroneous image model may corrupt the image information incorporated into the tracking method.

In this paper we present an improved method that solves the issue of a complex and dynamic background by integrating a Blind Source Separation (BSS) technique. The proposed approach consist in a detection step which uses the BSS results, followed by a tracking procedure which proceeds by joint estimation of the kinetic models of targets and the image model. Instead of using the original images, the tracking algorithm processes images where the background has been cancelled thanks to the BSS method. The BSS technique is derived from the Morphological Component Analysis (MCA) algorithm [8]. To adapt the MCA to the characteristics of fluorescent biological images, we modify it to incorporate different sparsity priors, impose a positivity constraint and define appropriate representation dictionaries for biological fluorescent images. We show that this algorithm successfully separates sources with different morphologies in microscopy images.

We detail in Section 2 the adaptations of the MCA algorithm to fluorescent biological images. In Section 3 we describe the detection and tracking procedure. Particle tracking results in highly complex background are given for plant cell images.

2. BLIND SOURCE SEPARATION FOR FLUORESCENSCE MICROSCOPY IMAGES
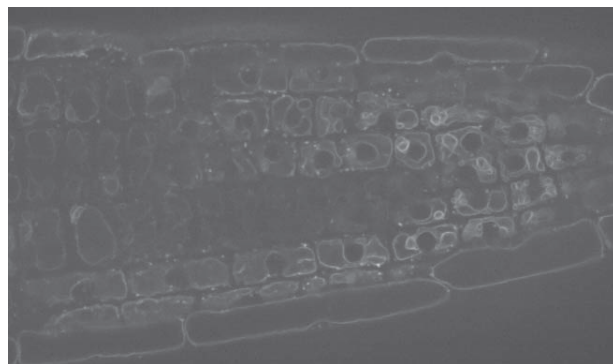
Fig. 1. A GFP KOR1 protein labeled vacuoles membranes and small compartments.

2.1. MCA with positivity constraints

The aim of blind source separation techniques is to recover the set of sources $S = [s_1^T, ..., s_n^T]$ from the observation of their mixture:

$$Y = AS + N, \tag{1}$$

where A is the mixture coefficients matrix, Y is the measured signal and N is the matrix containing measurement noise and model error. While well known Independent Component Analysis methods [9] rely on statistical principles, very recently some methods based on morphological diversity and sparsity have emerged [8]. They require the definition of a dictionaries set such that each source can be represented in a very sparse way in a given waveform dictionary of the set and in a very non-sparse manner in every other. In the case of noisy measurements, a signal s_i is said to be sparse in a waveform dictionary D_i if it can be represented from a very few dictionary elements: $s_i = \alpha_i D_i$, where most of the coefficients α_i are nearly zero.

The MCA algorithm [8] was primarily designed for the analysis of natural images and astronomical data. It decomposes the signal Y in a union of over-complete dictionaries using a modified block coordinate relaxation method which minimizes iteratively the following score function:

$$\min_{\{\alpha_i\}_{1...n}} \left[\sum_{i=1}^{n} ||\alpha_i||_0 + \lambda ||Y - \sum_{i=1}^{n} \alpha_i D_i||_2^2 \right]. \tag{2}$$

The first term of the sum reflects a sparsity constraint while the second term is the reconstruction error and introduces a data-driven constraint. The optimization algorithm proposed in [8] relies on an iterative alternate projection and thresholding scheme: the representation in a waveform dictionary is built while other sources are fixed.

In order to separate small particles, whose tracks are wanted, from background in biological images, we propose to use the MCA algorithm whereby particles are considered as one source and background structures as other sources. In fluorescence images a source physically generates photons that may be captured by the sensor. Hence a fundamental property of such images is the positivity of sources: $\forall i \; s_i > 0$. Consequently we aim at finding the representation $\{\alpha_i\}_{1...n}$ that maximizes the MCA score (Eq. 2) under the constraint: $\alpha_i D_i > 0$. Following ideas in [10] we enforce positivity by replacing negative values of a reconstructed source $\alpha_i D_i$ by zeros in the alternate MCA scheme. Enforcing the positivity constraint in the BSS procedure reduces negative representation errors such as ringing artifacts and we therefore expect a better separation of sources and an easier localization of particles.

2.2. Sparsity priors

The MCA score function is intricately related to a Maximum Likelihood formulation where the likelihood of the image representation is written as:

$$p(\{\alpha_i\}_{1...n}|Y) = p(\{\alpha_i\}_{1...n})p(Y|\{\alpha_i\}_{1...n})p(Y)^{-1} \tag{3}$$

Following the source mixture model (Eq. 1) we compute the image conditional probability $p(Y|\{\alpha_i\}_{1...n})$ as the probability of the residual between the observed image and the sources mixture. The residual should follow the same distribution as the noise N, hence under the assumption of white and Gaussian noise with zero mean and standard deviation σ we write:

$$p(Y|\{\alpha_i\}_{1...n}) = (2\pi\sigma^2)^{(-n/2)} \exp(-||Y - \sum_{i=1}^{n} \alpha_i D_i||_2^2/2\sigma^2). \tag{4}$$

Maximizing the representation log likelihood therefore results in:

$$\max_{\{\alpha_i\}_{1...n}} \ln(p(\{\alpha_i\}_{1...n}|Y))$$
$$= \max_{\{\alpha_i\}_{1...n}} \left[\ln(p(\{\alpha_i\}_{1...n})) - ||Y - \sum_{i=1}^{n} \alpha_i D_i||_2^2/2\sigma^2 \right]. \tag{5}$$

So by relating Equations 2 and 5 we deduce that minimizing the MCA score function is similar to maximizing the representation log likelihood, where:

$$p(\{\alpha_i\}_{1...n}) = \beta^{-1} \exp(-\beta^{-1} \sum_{i=1}^{n} ||\alpha_i||_0), \tag{6}$$

and: $\lambda = \dfrac{\beta}{2\sigma^2}$.

The probabilistic distribution $p(\{\alpha_i\}_{1...n})$ defined above corresponds to an exponentially distributed sparsity prior of mean β. When the only prior is the mean sparsity β The Maximum Entropy (MaxEnt) principle [11] dictates to choose a prior distribution of the form $Cr^{||\alpha_0||}$, with C and r fixed, which can be shown to tend to the exponential distribution defined in Equation 6 when each $||\alpha_i||_0$ and the size of the dictionaries exceed few hundreds. The exponential implicit choice of $p(\{\alpha_i\}_{1...n})$ in the MCA is therefore supported by the MaxEnt principle

In Equation 6 the expected sparsity is implicitly assumed equal for each dictionary of representation. However, in particles tracking applications we intend to separate particles, that are small, from background structures that are generally bigger and a much more complex signal. Hence in this case the sparsity of the source representing particles is expected to be much lower than the sparsity of sources containing other structures. In this case the standard prior probabilistic distribution (Eq. 6) is not proper since we expect very different sparsity values for sources. We therefore propose to define as many prior distributions as the number of sources instead of defining only one prior:

$$p(\alpha_i) = \beta_i^{-1} \exp(-\beta_i^{-1} ||\alpha_i||_0), \tag{7}$$

for $i = 1..n$. Here β_i is the expected sparsity for the coefficients α_i in the waveform dictionary D_i. Following the ML formulation (Eq. 5) of the MCA inverse problem we rewrite the original score function:

$$\min_{\{\alpha_i\}_{1...n}} \left[\sum_{i=1}^{n} \lambda_i^{-1} ||\alpha_i||_0 + ||Y - \sum_{i=1}^{n} \alpha_i D_i||_2^2 \right] \tag{8}$$

where: $\lambda_i = \dfrac{\beta_i}{2\sigma^2}$, for $i = 1..n$.

Maximizing the proposed score function (Eq. 8) is still feasible with the MCA iterative alternate projection and thresholding scheme by each time replacing the parameter λ by λ_i, that corresponds to the source currently processed.

2.3. Dictionaries set for biological images

In many fluorescence biological images small particles appear as nearly Gaussian spots since the point spread function of the acquisition system has a multidimensional Gaussian like shape [12]. We therefore propose the Undecimated Discrete B3-Wavelet Transform (UDWT) [13] as the waveform dictionary D_1 for this source, since it is built from nearly Gaussian functions. The dictionary D_2, that represents the background, must also be selected according to its

822

morphology. The non isotropic background in fluorescence images is often composed of linear structures, such as membranes and filaments. The Discrete Curvelet Transform (DCvT) [14] represents C^2 smooth curves optimally in 2d, hence it is well indicated for representing these signals. For images in which the background looks like texture, the Discrete Cosine Transform (DCT) is an appropriate dictionary because it models locally periodic signals in a sparse way. These three dictionaries have very fast implementations of direct and inverse transforms in 2d, which makes MCA computationally feasible.

An example of MCA capabilities when it is applied with an appropriate set of dictionaries is presented now. Figure 1 shows an image of epidermal root cells of Arabidopsis plants. The seedlings expressed the Green Fluorescent Protein (GFP) fused to the KOR-RIGAN1 (KOR1) protein. In order to study KOR1 compartments movements, a sequence of 20 images was acquired with a disk scanning confocal microscope. We apply here the proposed MCA procedure because signals of KOR1 proteins in compartments appear as small isotropic spots superposed to signals of membranes of vacuoles. Two dictionaries were consequently selected: UDWT for spots and DCvT for membranes. Here the DCT is useless because of the lack of texture in these images. The separation of compartments and membranes signals is very well achieved as shown in Figure 2.
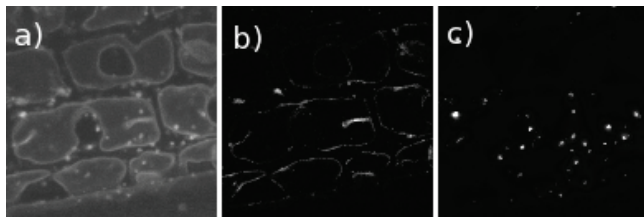
Fig. 2. Source separation in a fluorescent image: a) original crop, b) curvelet part $\alpha_2 D_2$, c) wavelet part $\alpha_1 D_1$.

3. PARTICLE TRACKING IN COMPLEX BIOLOGICAL ENVIRONMENT

3.1. Particle localization

We propose to detect small particles by analyzing the wavelet coefficients resulting from the BSS technique presented above and then follow them through time with a kinetic Bayesian tracking algorithm. In the following we call this combined BSS-detection method MCA-UDWT. One or few wavelet scale coefficients of the MCA are selected according to the particles sizes. A binary mask of each slice of the original image is obtained from the binarization of these coefficients by thresholding. The mask is used to obtain positions of individual particles by connected components extraction. In the case of the biological images presented in Section 2.1 the second wavelet scale of the resulting from the MCA is analyzed since it corresponds to the size of KOR1 compartments.

We compare the MCA-UDWT detection performance to those of a standard method consisting in thresholding the second scale of UDWT coefficients without BSS, and then extracting detections in a similar way as described for MCA-UDWT. In Figure 3 the scale 2 of MCA-UDWT and UDWT are depicted. It shows that there no longer remains any linear structure in the second scale given by MCA-UDWT filtering, which makes the detection process much more easier than in the second scale of UDWT which contains many linear
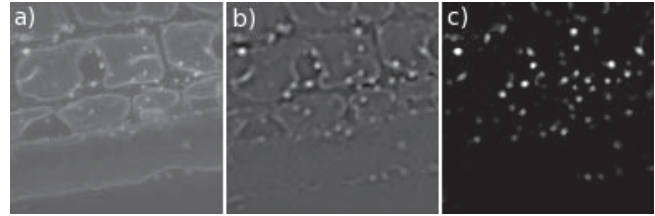
Fig. 3. (a) Original image. (b) 2nd scale of UDWT, (c) 2nd scale of MCA-UDWT.
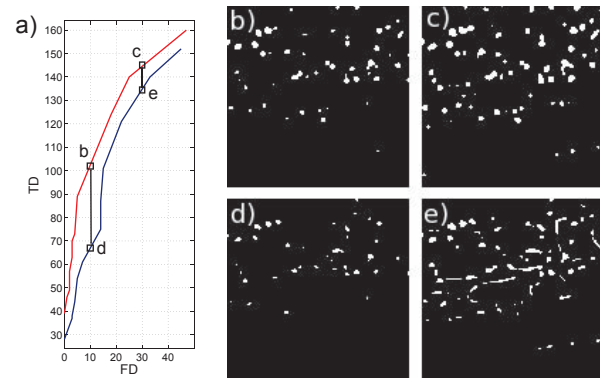
Fig. 4. a) Detection performance based on MCA-UDWT (red) and UDWT (dark blue). We note FD the number of false detections and TD the number of true detections. b) and c) are the binary images obtained by applying two different thresholds to the MCA-UDWT second scale, while d) and e) are the binary images obtained by applying two different thresholds to the UDWT second scale. Corresponding detection performance is indicated on the curves a).

residues.

corresponding binarized images clearly highlight this fact.

In order to assess quantitative results, an expert identified 303 spots in the three first frames of the sequence corresponding to this crop. Figure 4 represents the number of recovered detections and the number of false detections for various strategies of thresholding second scales coefficients. It shows that MCA-UDWT always recovers a higher number of targets than UDWT for a given number of false detections. As shown by the corresponding binary images, when only few detections are allowed the MCA-UDWT is more sensible than UDWT, while when more false detections are allowed the MCA-UWT detects some membranes.

3.2. Tracking of particles with joint kinetic and image estimation

Once the detection step has been performed detections have to be linked to build tracks. We adopt the unified Bayesian framework proposed in [7] in which the targets motion and the image model are combined in a joint likelihood of association. The kinetic information is computed thanks to a Kalman filtering derived technique and using multiple models of motion [15]. On the other hand the appearance likelihood relies on the description of a statistical model of image generation. Instead of using the original image model, we propose to use the image model I, where the background has been

823

cancelled thanks to the BSS results:

$$I = Y - \alpha_2 D_2 = s_1 + N = \sum_{j=1..m} p_j + N, \qquad (9)$$

where $\{p_j\}_{j=1..m}$ is the set of intensity profiles of the m particles found in the image. It is worth to note in Equation 9 that the acquisition noise N is not modified by the BSS process and the background subtraction since the MCA models its presence. Hence the tracking algorithm can use its probabilistic distribution to score the match between the observed image and associations between tracks and detections as done in [7].

In Figure 5a we show that the proposed tracking procedure is able to track particles that interact with membranes, while no false tracks originate from some spurious detections produced by the background. As originally proposed in [7] the appearance model is also used to separate closely spaced targets that appear fused due to the resolution limit thanks to the exploitation of the kinetic and image information. In Figure 5b and c the recovery of the aggregation of three particles is correctly processed despite the close proximity of membranes.

These results are opening new perspectives for biological studies: we are able to track particles in a very complex environment and also to quantify interactions with background structures since each separated image gives information about positions and dynamics of a source.
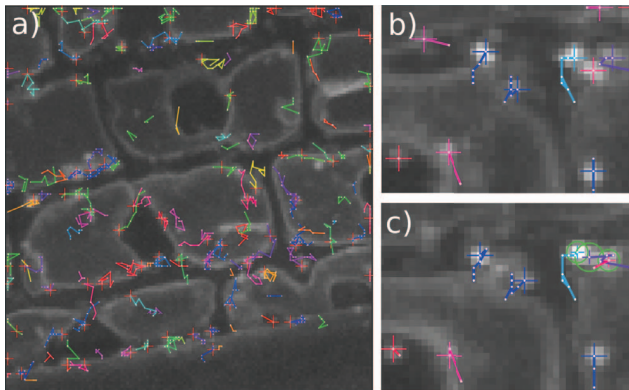
Fig. 5. a) Tracking numerous particles in plant cells with the proposed procedure. b) Detail of closely spaced particles, c) Recovery of the aggregation of three particles. Targets profiles are represented by green circles.

4. CONCLUSION

In order to address the issue of detecting and tracking particles in a complex background, we have adapted a source separation to the characteristics of fluorescent biological images. We have used the MCA algorithm that is based on sparsity principles, but we modified it to incorporate different sparsity priors, impose a positivity constraint and define appropriate representation dictionaries for biological fluorescent images. We showed that the proposed procedure successfully separates sources with different morphologies in microscopy images. Consequently, we have proposed an approach to detect and track particles that exploits the source separation results. The tracking algorithm is able to resolve particles that temporarily

aggregate by exploiting the new model of image in which the background has been cancelled. Moreover, we proved in a real case the ability of the method to track numerous particles in a complex and dynamic background, something which was not feasible until now, hence offering new tools to document interactions between cellular compartments.

5. REFERENCES

[1] J.-C. Olivo-Marin, "Extraction of spots in biological images using multiscale products," *Pattern Recognition*, vol. 35, no. 9, pp. 1989–1996, 2002.

[2] D. Thomann, D.R. Rines, P.K. Sorger, and G. Danuser, "Automatic fluorescent tag detection in 3D with super-resolution: application to the analysis of chromosome movement," *Journal of Microscopy*, vol. 208, no. 1, pp. 49–64, October 2002.

[3] I. Smal, M. Loog, W.J. Niessen, and E. Meijering, "Quantitative comparison of spot detection methods in live-cell fluorescence microscopy imaging," in *IEEE International Symposium on Biomedical Imaging*, June 2009.

[4] A. Genovesio, T. Liedl, V. Emiliani, W.J. Parak, M. Coppey-Moisan, and J.-C. Olivo-Marin, "Multiple particle tracking in 3D+T microscopy: methods and application to the tracking of endocytosed quantum dots," *IEEE Transactions on Image Processing*, vol. 15, no. 5, pp. 1062–1070, 2006.

[5] I. Smal, E. Meijering, K. Draegestein, N. Galjart, I. Grigoriev, A. Akhmanova, M. E. van Royen, A. B. Houtsmuller, and W.J. Niessen, "Multiple object tracking in molecular bioimaging by rao-blackwellized marginal particle filtering," *Medical Image Analysis*, vol. 12, no. 6, pp. 764–777, 2008.

[6] N. Chenouard, I. Bloch, and J.-C. Olivo-Marin, "Multiple hypothesis tracking in microscopy images," *IEEE International Symposium on Biomedical Imaging*, pp. 1346–1349, June 2009.

[7] N. Chenouard, I. Bloch, and J.C. Olivo-Marin, "Feature-aided particle tracking," in *Proceedings of the IEEE International Conference on Image Processing*, San Diego, Oct. 2008, IEEE.

[8] J.-L. Starck, M. Elad, and D.L. Donoho, "Redundant multiscale transforms and their application for morphological component analysis," *Advances in Imaging and Electron Physics*, vol. 132, 2004.

[9] J.-F. Cardoso, "Blind signal separation: statistical principles," *Proceedings of the IEEE*, vol. 86, no. 10, pp. 2009–2025, 1998.

[10] J.-L. Starck, J. Fadili, and F. Murtagh, "The undecimated wavelet decomposition and its reconstruction," *IEEE Transactions on Image Processing*, vol. 16, no. 2, pp. 297–309, Feb. 2007.

[11] E. T. Jaynes, *Probability Theory: The Logic of Science*, Cambridge University Press, April 2003.

[12] B. Zhang, J. Zerubia, and J.-C. Olivo-Marin, "Gaussian approximations of fluorescence microscope point-spread function models," *Applied Optics*, vol. 46, no. 10, pp. 1819–1829, Apr. 2007.

[13] J.-L. Starck, F. Murtagh, and A. Bijaoui, *Image processing and data analysis: the multiscale approach*, Cambridge University Press, 2000.

[14] E. J. Candes, L. Demanet, D. L. Donoho, and L. Ying, "Fast discrete curvelet transforms," *SIAM Journal on Multiscale Modeling and Simulation*, vol. 3, pp. 861 – 899, 2006.

[15] H. A. P. Blom and Y. Bar-Shalom, "The interacting multiple model algorithm for systems with markovian switching coefficients," *IEEE Transactions on Automatic Control*, vol. 33, no. 8, pp. 780–783, August 1988.